



NASA Public Access

Author manuscript

Colloids Surf A Physicochem Eng Asp. Author manuscript; available in PMC 2021 January 20.

Published in final edited form as:

Colloids Surf A Physicochem Eng Asp. 2019 January 5; 560: 136–140. doi:10.1016/

j.colsurfa.2018.10.019

Topological Control of Polystyrene-Silica Core-Shell Microspheres

Zane A. Grady¹, Alexandria Z. Arthur¹, Christopher J. Wohl²

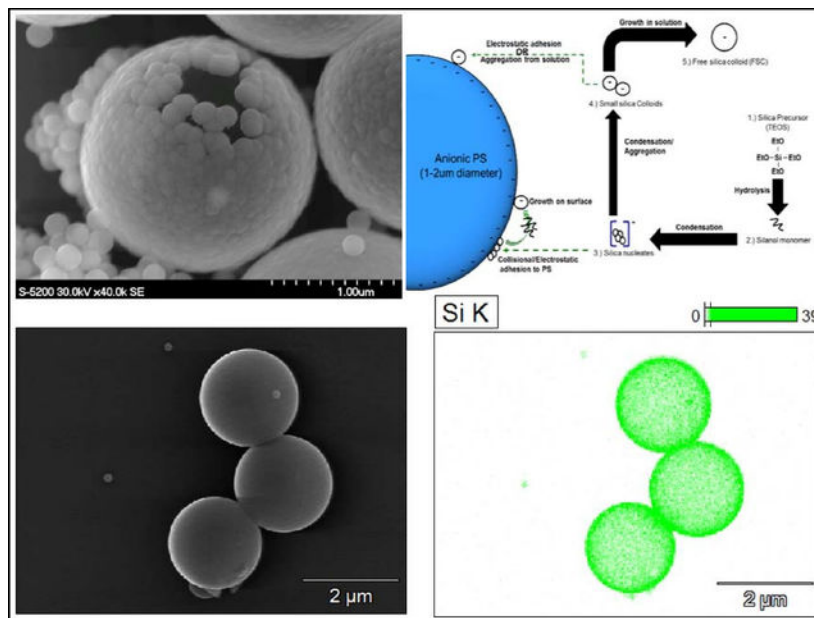
¹NASA Internships, Fellowships, and Scholars, NASA Langley Research Center, Hampton, VA 23681, USA

²NASA Langley Research Center, Hampton, VA 23681, USA

Abstract

Controllable surface morphology is requisite across a gamut of processes, industries, and applications. The surface morphology of silica-coated polystyrene microspheres was controllably modified to enable generation of both smooth and bumpy, or raspberry-like, surfaces. Although smooth and raspberry-like silica shells on polystyrene templates have been demonstrated extensively, the method described here used readily available materials to produce radical changes in surface morphology from a single polystyrene template coated in silica through a facile sol-gel reaction processes. Silica shells were deposited via a sol-gel process (using tetraethyl orthosilicate as the silica precursor) onto 1 to 2 μm diameter anionic polystyrene spheres, fabricated by emulsifier-free polymerization. By varying of the concentration of silica precursor and ammonium hydroxide catalyst and altering the electrostatic surface interactions via addition of a cationic polymeric brush, an array of surface topologies was generated. The resulting silica shells ranged from 100 to 200 nm in thickness, as measured by calcination of the polystyrene template. Empirical relations between reaction conditions and the resulting silica colloid diameter were utilized to understand the resultant silica shell topology. These results may serve as a guide to generate a versatile platform for research in the multitude of applications where polystyrene-silica core-shell particles are utilized.

Graphical Abstract



Keywords

core-shell particles; sol-gel; surface topology

Introduction

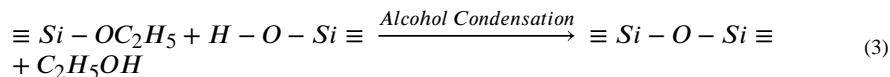
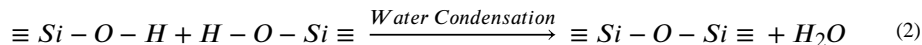
Core-shell hybrid particles are attractive for many applications due to their material combinations, versatility, and microstructural variability. In particular, the polystyrene (PS) core – silica shell (SS) system has been a subject of research for decades, as they are a precursor for hollow silica shell nanoparticles (HSSN),^{1–8} or further functionalized for applications in immunoassay,⁹ macro-regime self-assembly,¹⁰ and targeted drug delivery.^{2, 6–7, 11}

Geometric and microstructural properties of PS-SS are often optimized for a specific application. For example, tunable superhydrophobic surfaces from deposited particulate monolayers necessitate hierarchical surface roughness,^{8, 12–16} so raspberry-like hybrid particles in the sub-micrometer regime are desired. Conversely, in applications where a smooth sphere is preferred,^{1, 17–18} a smooth silica shell is advantageous. Likewise, a mesoporous shell is favorable in applications where an encapsulated substance must be infiltrated/released. Lastly, a non-porous shell is preferable for applications focused on mechanical integrity¹¹ or further shell surface functionalization.

This study was conducted to build on the foundation laid by Werner Stöber's seminal work on monodisperse silica colloid synthesis, which introduced a new field of research on sol-gel synthesized materials.¹⁹ Many groups have previously presented facile methods to synthesize PS-SS hybrid particles with tunable porosity, shell thickness, and topology. The previously published results described shell formation processes via a sol-gel reaction in the presence of previously synthesized PS spheres. The PS templates vary in surface charge

(cationic^{1-2, 4-7, 14, 18, 20-22} or anionic^{2, 17, 23-24}) and diameter (nanometer^{1-4, 6-7, 11, 13, 17, 20-21, 23-26} to micrometer^{5, 9, 15, 18}). Various theories have been presented to elucidate the shell formation process that attempt to link silica nanoparticle genesis via the sol-gel process with proposed PS template interactions.^{25, 27-28} Currently, there is a consensus on a prevailing theory of silica shell growth via the sol-gel process. This debate contrasts whether the sol-gel process resulting in shell growth can be more accurately described by a monomer-addition growth theory²⁹, or a controlled aggregation theory.³⁰⁻³² In other words, does silica nucleation occur in the early stages of the reaction followed by an extended period of growth, or does nucleation and growth occur concurrently throughout the duration of the reaction? Previous attempts to unite the theoretical understanding of silica shell growth with the sol-gel process have culminated in predictive models of shell growth.^{7, 17} However, there exists no model which spans the nanometer to micrometer regimes that accounts for the variety of systematic changes that previous work, and this current research introduce. In this study, a series of PS-SS materials was generated under different reaction conditions. The topology of synthesized PS-SS materials was characterized and compared to prominent models for silica particle and shell growth.

The silica sol-gel reaction, reviewed in detail recently by Rahman et al,³² occurs through hydrolysis of the silica precursor (1), followed by either water (2) or alcohol condensation (3).



Hydrolysis of tetraethyl orthosilicate (TEOS) produces free silanol groups, which readily link with other silanol groups or ethoxy groups forming Si-O-Si bridges that characterize the final silica structure. Stöber and Fink are attributed with pioneering the study of creating monodisperse particles with this modifiable sol-gel process.¹⁹ The majority of silica shell coating procedures, including this one, employ the Stöber method. A general description of this process is shown in Scheme 1. First, the silica precursor is hydroxylated via a basic solution to create free silanol monomer. Second, these monomers condense to form small anionic silica nucleates, which may either deposit onto the template (PS) surface or further condense with additional silanol monomer. Third, the silica nucleates grow to become colloids, until reaching an equilibrium radius, which is dependent on the reaction conditions. Finally, the mature silica colloids are then either deposited onto any remaining free template surface or stabilize in solution (i.e. free silica colloids). The topology of the resulting shell is determined by the size of the silica nucleates/colloids that participate in shell formation as well as the ability of the silica nucleates/colloids to absorb silica monomer once adhered to the PS surface. Smooth shells are formed when the reaction environment favors generation

of numerous small silica nucleates which adhere to the PS template resulting in uniform shell growth. Raspberry-like (bumpy) silica shells are generated when nucleates grow into large colloids that subsequently adsorb to the polystyrene surface. This results in shell formation at later stages in the sol-gel process.

Prior work has examined the influence of surface charge, pH, reaction time, and additives on resultant shell topology.^{10, 15, 20–21, 23} In this study, negatively charged PS microspheres (1.5–2 μm) were coated with silica via a sol-gel process using TEOS as the silica precursor and ammonia (generated from ammonium hydroxide) as the reaction catalyst, in an aqueous ethanol solution. TEOS and ammonia concentration, the surface charge of the PS template, and the method of reactant introduction were varied. The influence these changes had on particle morphology was investigated using high-resolution scanning electron microscopy (HRSEM). With the exception of PS template surface charge, all reaction variables were chosen to influence the kinetics of the sol-gel process. This study addressed previously cited problems such as incomplete shell generation in the micrometer regime, free silica colloid (FSC) genesis,¹⁰ dependence on additives that increase reaction cost/complexity, and conditions generating particle surface morphologies.

Experimental Methods and Materials

Polystyrene Microparticle Preparation

Anionic 1.5–2 μm polystyrene microspheres were synthesized by soap-free emulsion polymerization (SFEP) of styrene (freshly distilled to remove the t-butyl catechol inhibitor) initiated with potassium persulfate (KPS) (both obtained from Sigma Aldrich).³¹ Magnesium sulfate (MgSO_4) was included to control the PS microsphere final diameter. The particles were centrifuged at 4500 RPM twice with deionized water and once with methanol to remove unreacted monomer and soluble oligomeric species, followed by freeze drying (Flexi-Dry MP) of the remaining purified PS microparticles.

Experiments utilizing cationic surface charged PS were functionalized with poly diallyldimethyl ammonium chloride (PDADMAC), as follows: 3 g of freeze-dried PS microparticles were suspended in 300 mL of 98 volume % ethanol/deionized (DI) water solution. The mixture was sonicated at room temperature for 10 minutes and stirred vigorously using a magnetic stir bar. 3.6 g of PDADMAC (ratio: 1.2 g PDADMAC per 1 g PSM) was added to the solution, which was subsequently stirred for 12 hours at room temperature. The solution was then centrifuged (4500 RPM) twice with DI water and once with methanol for 10 minutes, followed by freeze drying. The PDADMAC-coated particles were subsequently utilized for the same silica coating process as described below.

Silica Shell Generation

Silica coating was carried out via a one-pot sol-gel reaction utilizing tetraethyl orthosilicate (98% TEOS, Acros Organics) as silica precursor and ammonium hydroxide (NH_4OH , Fisher Scientific) as the source for the base-catalyst, ammonia. The sol-gel reactions were performed in a round bottom flask with a magnetic stir bar. The freeze-dried PS microspheres were dispersed into a 98 vol. % ethanol-deionized (DI) water solution at a

concentration of approximately 100 ml solution: 1 g PS microspheres. The suspended PSM solution was then sonicated for ten minutes to break up aggregates, and subsequently placed in an 70°C oil bath, with the reaction mixture being vigorously stirred. TEOS and ammonium hydroxide were added in quick succession, and a water cooled condenser was placed on the reaction vessel. The mixture was allowed to stir for 6 hours at 70 °C, followed by 12 hours without heat. Next, the silica-coated particles were centrifuged for 10 minutes at 4500 rpm and washed twice with deionized water and once with methanol. The particles were sonicated for 10 minutes at room temperature prior to each centrifugation. The cleaned particles were then freeze-dried for at least 4 hours.

The following procedure was utilized to observe the progress of silica shell formation. After allowing the reaction solution to stir in solution for 30 minutes, 5 mL of the solution was removed via pipet and charged into a small glass vial. The vial was then immediately chilled in a dry ice/isopropanol bath for 5 minutes. Next, the solution was centrifuged at 4500 RPM for 5 minutes, and the supernatant removed. The particles were then re-dispersed in DI water and this solution was centrifuged according to the previously described conditions. This process was completed a total of 3 times, followed by a final centrifuge/rinse cycle in methanol.

Microscopy samples were prepared by dispersion of particles on a pure carbon film 200 mesh TEM grids (Ted Pella, Inc.). The solvent was allowed to evaporate prior to imaging. The samples were imaged optically (Leica DFC450) and with an HRSEM (Model S-5200, Hitachi). All electron dispersive mapping (EDS) was carried out using a Thermo Scientific Noran System 7.

Results

The effect of sol-gel reaction parameters (silica precursor and catalyst concentration), PS core functionalization, incremented addition of reactants on the particle-shell assembly process, and final topology were investigated. The following results detail the observed effects of each distinct variable. Finally, a discussion of raspberry-like versus smooth shell formation processes is presented.

Effect of silica precursor concentration

All reactions discussed in this section were carried out in one-pot (no incremental addition) processes, unless otherwise stated. One approach to changing the resultant shell morphology was to vary the concentration of TEOS silica monomer. From 3 mL TEOS / 1 g PS to 15 mL TEOS / 1 g PS. Incomplete silica shells were formed at low TEOS concentrations (Fig. 1.A). TEOS ratios of 6–7.5 mL TEOS / 1 g PS generated sufficient amounts of silica monomer to form raspberry-like shells, without generation of noteworthy colloid growth/networking. At high TEOS concentrations, intra-particle silica bridging was observed (Fig1.D). Without modifying the PS surface chemistry with any cationic brush, the negatively charged silica sols were repelled from surface adhesion, and preferentially grew in solution. Therefore, regardless of TEOS concentration, formation of a silica shell would only arise after silica particle growth had advanced enough to overcome this initial repulsive interaction.

While varying the concentration of TEOS was sufficient to tune morphology in the sub-micrometer sized regime (diameter < 750 nm),⁴ it was insufficient for targeted modification in the 1–2 μm particle functionalization. As shown figures 1.B–C, silica shells formed at 6 mL TEOS / 1 g PSM were slightly less raspberry-like (i.e., smoother morphology) than particles generated at 7.5 mL TEOS/1 g PSM. However, even under these conditions, incomplete shell formation was observed. As reactions with 6 mL and 7.5 mL TEOS/g PSM generated elevated levels of colloidal silica in solution, further system modification to obtain targeted morphologies, while mitigating free silica colloid genesis, were necessary.

Effect of ammonium hydroxide concentration

Previous studies have identified an ideal pH range of 10–11, noting that solutions with pH values significantly different from this range are unsuitable for shell formation.³³ All samples were prepared with a TEOS concentration of 6 mL TEOS/1 g PS microspheres, previously shown to be suitable for shell formation. Ratios of ammonium hydroxide-derived ammonia to TEOS were investigated ranging from 0.5–2.0 mL NH_4OH /1 mL TEOS. The prepared solutions of 1 mL NH_4OH /1 mL TEOS had pH values from 10–12, producing silica shells of raspberry-like morphologies (Fig 1.B). Therefore, this ratio was used as the baseline NH_4OH /TEOS ratio for all experiments. Halving the baseline catalyst concentration to 0.5 mL NH_4OH /1 mL TEOS resulted in no shell formation as seen in Figure 2.A. This occurred from the pH lying outside the ideal silica forming range (10–11). Doubling the baseline catalyst concentration to 2 mL NH_4OH /1 mL TEOS resulted in complete raspberry-like shell formation, with silica colloids both adhered to the PS microspheres and freely in solution. These colloids were on average 40 nm larger than those observed under the baseline conditions (Fig 2.A).

These results (i.e., solution pH values considerably lower than 10 are inadequate for shell formation) are comparable to those reported for silica shell formation on smaller sized particles.³⁴ Furthermore, increased concentration of NH_4OH resulted in exaggeration of the raspberry-like shell morphology observed under baseline conditions. The increased surface roughness from increasing amounts of catalyst was the consequence of larger silica colloid present during shell formation.

As was concluded by Rahman et al.,³² smaller silica nanoparticles are produced under slower reaction rate conditions, primarily achieved by decreasing the concentration of base-catalyst. However, based on the results from the experiments described here, reducing the ammonium hydroxide concentration resulted in incomplete silica shell formation. The apparently smooth silica shell observed in Figures 2.A–B was likely due to random collisions between silica nucleates and the PS template surface, not the result of undergoing shell formation. This is supported by the low concentration of NH_4OH present and the lower relative magnitude of Si K count value (a measure of signal strength from EDS measurements) measured for these materials, compared to those observed from imaging samples prepared from high base-catalyst concentration reactions. The Si K count ranges for batches prepared with 1 and 2 mL NH_4OH /1 mL TEOS were 46 and 58, respectively. Increasing the base-catalyst concentration has been shown to favor nucleate growth via silanol absorption.^{7, 17} These silica particle growth-favored reactions resulted in larger silica

particle formation and, for the cases discussed here, generation of a bumpy raspberry-like silica shell morphology. Thus, varying the concentration of ammonium hydroxide relative to TEOS effectively controls the rate of TEOS hydroxylation and subsequent silica particle growth, which indirectly influences the topology of the resulting silica shell. Unfortunately, varying this ratio though, was not sufficient to enable generation of a continuous, smooth silica shell.

Effect of poly(diallyldimethyl ammonium chloride)

Modifying the surface of PS microparticles with PDADMAC was successful in promoting silica nucleate adhesion to the PS surface in the early stages of silica growth, resulting in smooth silica shells. Initially, PDADMAC was introduced simultaneously with the TEOS, the results of which are shown in Fig.3 A–B. Based on the bumpy morphology of the resultant silica shell, it was determined that PDADMAC present in solution, i.e., not associated with PS microspheres, increased the number of nucleates. This resulted in asymmetric and colloid decorated silica shells (Fig.3 A–B).

Smooth silica shells were obtained when the excess PDADMAC was removed from the PSM solution prior to silica coating (Fig.3 C–D). By inducing electrostatic attraction between silica nucleates and PSM, the sol-gel reaction could occur preferentially on the surface of the PSM. This surface-favored nucleation and growth resulted in formation of exceptionally smooth silica shells, and relatively few silica colloids in the surrounding solution. Although there appeared to be fewer free silica colloids in the cationic PS system compared to typical anionic PS systems, the observed colloids appeared to grow to significantly larger diameters (Fig.3. C–D). This was likely due to residual PDADMAC in solution interacting with silica nucleates, followed by aggregation of silica sols into the larger colloids.

Effect of incremental addition

Distributing reactant introduction over longer periods of time, limiting the available TEOS to react, has been previously shown to produce smaller silica nanoparticles.³³ Therefore, addition of reactants (TEOS) at discrete increments was investigated to determine if this approach would result in generation of smooth silica shell formation with little to no free silica colloid genesis. For these experiments, TEOS and NH₄OH were added to PDADMAC-coated PSM under reactant ratios of 6 mL TEOS: 1 g PSM and 1.5mL NH₄OH: 1 mL TEOS. These conditions were identified that reproduce complete raspberry-like shells with minimal colloidal silica generation.

As a first attempt, the total TEOS added was separated into four equal addition steps completed at 30 minute intervals. Figure 4. A–B depicts the progressive growth of the silica shell after 2 increments of $\frac{1}{4}$ total reactant volume ($V = 2 * \frac{1}{4} V_{total} = \frac{1}{2}V_{total}$), and figure 4. C–D depicts shell growth after four $\frac{1}{4} V_{total}$ additions ($V = 4 * \frac{1}{4}V_{total} = V_{total}$). Smooth shell formation was observed in Fig.4 A–B after half of the total reactant volume had been introduced, suggesting that discretely introducing reactant fractions reduced the requisite TEOS for shell generation. After two additional reactant increments (Fig.4 C–D), a complete silica shell formed and excess silica colloids clustered on the surface of the PSM. This

result, small colloid generation on the surface of a smooth silica shell after two increments, was determined to be indicative of stable shell formation early in the synthesis with the later stages of the reaction resulting in colloid generation on the silica shell surface, instead of contributing to shell completion/thickening. It was therefore deduced that introducing the reactants in two increments optimized the generation of a smooth silica shell with little to no silica colloid generation.

To further evaluate this, a second TEOS addition scenario was evaluated where the total addition was separated into two increments consisting of 2/3 and 1/3 of the total TEOS, with the two reactant additions completed at 30-minute intervals. Silica shells generated from these experiments were determined to have a smooth topology and smaller/less numerous silica colloids (Fig.4 E–F), relative to the equal-volume four-increment counterpart (Fig.4 C–D). These results therefore demonstrated the ability to tune the thickness and morphology by segmentation of a naturally continuous sol-gel reaction.

Discussion

The behavior of silica shell formation on the PSM in these experiments deviated from that reported in the literature regarding shell formation on PSM's with smaller radii. At small length scales (template particle radii less than approximately 250 nm), the silica shell topology is driven by the nucleation and growth rate of the silica nucleates and colloids respectively. At larger length scales, factors such as electrostatic interaction at the PS-silica interface and discrete sol-gel growth stages appear to become significant. These microscale variables (tunable electrostatic surface functionalization and incremented reactant addition) offer a degree of control over the final shell topology that is absent from core-shell reactions in the sub-micrometer regime. Here, we attempt to collectively interpret the results from the distinct reaction series described in the preceding sections to guide future work in silica shell formation on PSMs within the micrometer-regime.

Smooth Shells

Congruent with previous research, raspberry-like (RL) shell topologies are preferentially created in the most commonly cited sol-gel reaction conditions. As detailed in these experiments, generating smooth shells requires careful selection of reaction conditions and functionalization of the template. Our studies have identified a narrow window of conditions which prefer formation of a smooth silica shell as opposed to a RL shell. Cationic functionalization proved to have the most significant impact on the resulting shell morphology. This was not the first instance of cationic functionalization of a PS core (poly vinylpyrrolidone^{4,9,18,20–23,25,37}, cetyl trimethylammonium bromide^{1–2,11,35}, etc.) but it was the first demonstration of the use of cationic functionalization in this size regime which enables tuning the degree of smoothness as well as thickness. We have not identified any variations in sol-gel reactant concentrations which could rival the smoothness in the shells produced atop PDADMAC-functionalized PS cores, however, it was possible that incremental addition of reactants onto an anionic PS system may produce smoother shells than observed in analogous one-pot syntheses. Previous work regarding the “seed method”

of sol-gel colloid growth is well documented^{27, 30–32}, so expansion of this approach to shell growth may yield interesting results.

Beyond functionalization of the PS core, the concentration of sol-gel reactants and increment-addition pattern appear to have secondary but not insignificant effects. As seen in Figure 3C–D, a reactant volume which might comfortably coat an anionic PS particle with a RL shell will coat a PDADMAC-coated particle with a thick smooth shell, decorated by large silica colloids. It stands to reason that the deposition efficiency of silica was increased when the particles attract, rather than repel, the negatively charged silica nucleates. This would also explain why fully formed, albeit thin, silica shells were observed upon addition of only half of the reactant volume during incremented reactions (Figure 4A–B).

Raspberry-Like Shells

Due to the naturally spherical nature of colloids grown by the sol-gel process, RL shells are the predominant shell topology formed. In order for the topology of the shells to become “tunable”, i.e. enable facile transition from RL to smooth, the diameter of the colloids must be much smaller than that of the PS template. If the silica particles approach the size of the deposition template, the RL-topology dominates solely because the shell is comprised of few, relatively large particles. This is commonly seen in the literature^{5, 8, 13–16, 21–22, 24–25, 27} where small template particles are used and the sol-gel process is carried out in conditions similar to those described here. Generation of smooth shells in these instances would most likely require either an unusually long reaction at a slow rate or creative functionalization of the template beyond simple surface charge modification.

Though RL shells are generated easily under many different reactant conditions, it has proven difficult to minimize the amount of free colloid contamination of both the solution and the PSM-Si shell surfaces. In many of our experiments which produced RL-shells, any degree of control over shell thickness or otherwise was negated by the lack of control over colloid contamination (figure 1C–D, figure 2C–D). The only identified method of reducing the number of resulting colloids was rigorous centrifugation. Samples taken at intermediate increments of the truncated reaction series of experiments, which were not centrifuged in an effort to best preserve the as-extracted state of the shells, exhibited a high degree of colloid contamination. This was not observed in the final centrifuged samples (figure 6). Further, attempts to decrease the reaction rate, and hopefully mitigate colloid generation, via reduction of catalyst concentration were unsuccessful in significantly addressing the colloid problem before the catalyst concentration was too low to form full shells.

While successful in the endeavor to reliably produce shells of desired topology in the micrometer-size regime, the present work also poses new questions and challenges. Perhaps most significantly, the underlying mechanics of the shell formation process remain elusive. Attempts to explain our results using theories of sol-gel reaction kinetics^{24,27,32}, models of PS-silica electrostatic interaction^{25, 28}, and models for shell formation on PS cores^{27, 20} were unsuccessful. While the mechanisms and kinetics of the silica sol-gel reaction are well understood, the largely empirical models proposed for shell growth via this process are lacking. A fuller understanding of the shell formation process may elucidate the staged shell growth observed in Figure 4A–D, where a quickly formed smooth silica shell appears to

resist the addition of further growth. Further, the shell formation in incremented reactions is sensitive to the relative volume of the reactions. This is not accounted for in the current understanding of shell formation. In-situ observation of shell growth in incremented reactions, as well as their analog sol-gel reactions sans particles, may reveal some of the intermediate steps to shell formation. These experiments would also benefit from examining the structure of the shells via calcination, which has been shown to be an effective mode of evacuating the organic PS core, allowing for observation of the internal structure. Following the calcination procedure described by Blas et al.² for calcination via an isothermal hold above 600°C, thermally calcined samples were generated (Figure 7). Measurements of the shell thickness and observations of the shell structure of the combusted particles also highlight the variability in shell formation of RL shells. The shells shown in Figure 7A–C were generated from a one-step sol-gel process with reactant proportions similar to trial 3 of Table 1. Nonetheless, the shells generated differ in thickness (the shell observed in Fig.7A is nearly twice that in Fig.7B) and internal structure (shells observed in Figs.7A and 7C are comprised of discrete colloids fused together, while the shell in Fig.7B appears continuous). A more complete understanding of the reaction kinetics and mechanisms responsible for the fusion versus stabilization of the silica colloids may offer more control over the characteristics of the RL shells.

Conclusion

Micrometer regime anionic PSMs combined with a TEOS/NH₄OH sol-gel reaction system were determined to yield a readily tunable range of silica shell topologies. Through manipulation of the sol-gel reaction on the PSM surface, the size and adhesive proclivity of the silica colloid may be altered to promote either smooth or raspberry-like topologies. Smooth shells were produced by sol-gel reactions which favor generation of small nucleates over growth of large colloids and by increased electrostatic attraction between nucleates and the PS surface. Practical application of these smooth shell parameters was determined to require surface functionalization of the anionic PS with a PDADMAC, which acted as a cationic coating. The smoothest shells were obtained when the PSM was PDADMAC-functionalized and the reactants were added in discrete increments. Two incremental additions of reactants were determined to be most favorable for a smooth shell with little to no silica colloid generation. The relative fractions of the total volume of each increment may be varied to tune the thickness of the resulting silica shell. Raspberry-like shells were formed under conditions where large silica colloids grew in solution and participated in shell growth at later reaction stages than under conditions resulting in smooth shell formation. Thus, generation of a smooth silica shell is achieved when the growing silica colloids are generated slowly (due to lower catalyst concentrations and lower available reactant, i.e., incremental addition) and when these small silica colloids are attracted to the PSM surface. Raspberry-like shell morphologies can be achieved by more rapid silica colloid growth (increased catalyst or reactant concentrations) and reduced attractive interaction between the colloid and the PSM surface. Under these conditions though, it is likely that a significant portion of silica colloids will be generated that are not closely associated with PSMs and care must be taken to separate these species. The resulting capacity to tune the morphology

of silica shells offers a wide range for future applications of polystyrene-silica core-shell microspheres.

References

1. Yeh Y-Q; Chen B-C; Lin H-P; Tang C-Y, Synthesis of Hollow Silica Spheres with Mesoporous Shell Using Cationic-Anionic-Neutral Block Copolymer Ternary Surfactants. *Langmuir* 2006, 22, pp 6–9. [PubMed: 16378389]
2. Blas H; Save M; Pasetto P; Boissiere C; Sanchez C; Charleux B, Elaboration of Monodisperse Spherical Hollow Particles with Ordered Mesoporous Silica Shells via Dual Latex/Surfactant Templating: Radial Orientation of Mesopore Channels. *Langmuir* 2008, 24 (22), pp 13132–13137. [PubMed: 18947208]
3. Bao Y; Shi C; Wang T; Li X; Ma J, Recent progress in hollow silica: Template synthesis, morphologies and applications. *Microporous Mesoporous Mater* 2016, 227, pp 121–136.
4. Shang Q; Zhou Y, Facile fabrication of hollow mesoporous silica microspheres with hierarchical shell structure via a sol-gel process. *J Sol-Gel Sci Technol* 2014, 75, pp 206–214.
5. Nandiyanto ABD; Iwaki T; Ogi T; Okuyama K, Mesopore-free silica shell with nanometer-scale thickness-controllable on cationic polystyrene core. *J Colloid Interface Sci.* 2013, 389, pp 134–146. [PubMed: 23058978]
6. Li D; Zhu Y; Mao C, One-pot synthesis of surface roughness controlled hollow silica spheres with enhanced drug loading and release profiles under ambient conditions in aqueous solutions. *J Mater Chem* 2013, 1, p 5515.
7. Nandiyanto AB; Akane Y; Ogi T; Okuyama K, Mesopore-Free Hollow Silica Particles with Controllable Diameter and Shell Thickness via Additive-Free Synthesis. *Langmuir* 2012, 28, pp 8616–8624. [PubMed: 22587437]
8. Liu S; Latthe SS; Yang H; Liu B; Yang R, Raspberry-like superhydrophobic silica coatings with self-cleaning properties. *Ceramics Int.* 2015, 41, pp 11719–11725.
9. Sarma D; Gawlitza K; Rurack K, Polystyrene Core-Silica Shell Particles with Defined Nanoarchitectures as a Versatile Platform for Suspension Array Technology. *Langmuir* 2016, 32, pp 3717–3727. [PubMed: 27018430]
10. Yu L; McLellan J; Xia Y, Synthesis and Crystallization of Hybrid Spherical Colloids Composed of Polystyrene Cores and Silica Shells. *Langmuir* 2004, 20, pp 3464–3470. [PubMed: 15875883]
11. Bai X; Xue C-H; Jia S-T, Surfaces with Sustainable Superhydrophobicity upon Mechanical Abrasion. *ACS Appl. Mater. Interfaces* 2016, 8, pp 28171–28179. [PubMed: 27668829]
12. Ming W; Wu D; van Bentem R; de With G, Superhydrophobic Films from Raspberry-like Particles. *Nano Letters* 2005, 5 (11), pp 2298–2301. [PubMed: 16277471]
13. Telford AM; Easton CD; Hawkett BS; Neto C, Waterborne, all-polymeric, colloidal ‘raspberry’ particles with controllable hydrophobicity and water droplet adhesion properties. *Thin Solid Films* 2016, 603, pp 69–74.
14. D’Acunzi M; Mammen L; Singh M; Deng X; Roth M; Auernhammer GK; Butta H-J; Vollmer D, Superhydrophobic surfaces by hybrid raspberry-like particles *Farad. Discuss* 2010, 146, pp 35–48.
15. Fan X; Zheng L; Cheng J; Xu S; Wen X; Cai Z; Pi P; Yang Z, Template synthesis of raspberry-like polystyrene/SiO₂ composite microspheres and their application in wettability gradient surfaces. *Surf. Coat. Technol.* 2012, 213, pp 90–97.
16. Fan X; Niu L; Wua Y; Chengb J; Yangb Z, Assembly route toward raspberry-like composite particles and their controlled surface wettability through varied dual-size binary roughness. *Appl. Surf. Sci.* 2015, 332, pp 393–402.
17. Hotta Y; Alberius P; Bergstrom L, Coated polystyrene particles as templates for ordered macroporous silica structures with controlled wall thickness. *J Mater Chem* 2003, 13, pp 496–501.
18. Hong J; Han H; Hong CK; Shim SE, A Direct Preparation of Silica Shell on Polystyrene Microspheres Prepared by Dispersion Polymerization from Polyvinylpyrrolidone. *J. Polym. Sci. Part A: Poly. Chem* 2008, 46, pp 2884–2894.

19. Stober W; Fink A, Controlled Growth of Monodisperse Silica Spheres in the Micron Size Range. *J Colloid Interface Sci.* 1968, 26, pp 62–69.
20. Kobayashi Y; Misawa K; Kobayashi M; Takeda M; Konno M; Satake M; Kawazoe Y; Ohuchi N; Kasuya A, Silica-coating of fluorescent polystyrene microspheres by a seeded polymerization technique and their photo-bleaching property. *Colloid Surf. Part A: Physicochem. Eng. Asp* 2004, 242 (1–3), pp 47–52.
21. Graf C; Vossen DLJ; Imhof A; Blaaderen A. v., A General Method To Coat Colloidal Particles with Silica. *Langmuir* 2013, 19, pp 6693–6700.
22. Zhang F; Xiao Z-Y; Zhai S-R; Zhai B; Yang P-F; An Q-D, PVP-Assisted Synthesis of Raspberry-Like Composite Particles. *J Sol-Gel Sci Technol* 2016, 78 (1), pp 228–238.
23. Zou H; Wu S; Ran Q; Shen J, A Simple and Low-Cost Method for the Preparatin of Monodisperse Hollow Silica Spheres. *J Phys. Chem. C* 2008, 112 (31), pp 11623–11629.
24. Du X; Liu X; Chen H; He J, Facile Fabrication of Raspberry-like Composite Nanoparticles and Their Application as Building Blocks for Constructing Superhydrophillic Coatings. *J Phys. Chem. C* 2009, 113 (21), pp 9063–9070.
25. Wang L; Song L; Chao Z; Chen P; Nie W; Zhou Y, Role of surface functionality on the formation of raspberry-like polymer/silica composite particles: Weak acid–base interaction and steric effect. *Appl. Surf. Sci.* 2015, 342, pp 92–100.
26. Takai C; Watanabe H; Asai T; Fuji M, Determine apparent shell density for evaluation of hollow silica nanoparticle. *Colloid Surf. Part A: Physicochem. Eng. Asp* 2012, 404, pp 101–105.
27. Rosu C; Selcuk S; Soto-Cantu E; Russo PS, Progress in silica polypeptide composite colloidal hybrids: from silica cores to fuzzy shells. *Colloid Polym. Sci.* 2014, 292, pp 1009–1040.
28. Chan AT; Lewis JA, Electrostatically Tuned Interactions in Silica Microsphere-Polystyrene Nanoparticle Mixtures. *Langmuir* 2005, 21, pp 8576–8579. [PubMed: 16142928]
29. Matsoukas T Silica particles from alkoxides: A spectroscopic study of particle formation and growth. Ph.D. thesis, University of Michigan, Ann Arbor, 1989.
30. Bogush GH; Zukoski CF, Uniform Silica Particle Precipitation: An Aggregative Growth Theory. *J Colloid Interface Sci.* 1991, 142 (1), pp 19–34.
31. Tiemsin P; Wohl CJ Refined Synthesis and Characterization of Controlled Diameter, Narrow Size Distribution Microparticles for Aerospace Research Applications. National Aeronautics and Space Administration, 2012, TM-2012–217591.
32. Rahman IA; Padavettan V, Synthesis of Silica Nanoparticles by Sol-Gel: Size-Dependent Properties, Surface Modification, and Applications in Silica-Polymer Nanocomposites—A Review. *J Nanomater.* 2012, 2012, pp 1–15.
33. Wu L; Jiao Z; Wu M; Song T; Zhang H, Formation of mesoporous silica nanoparticles with tunable pore structure as promising nanoreactor and drug delivery vehicle. *RSC Advances* 2016, 6, pp 13303–13311.
34. Lu Y; McLellan J; Xia Y, Synthesis and Crystallization of Hybrid Spherical Colloids Composed of Polystyrene Cores and Silica Shells. *Langmuir* 2004, 20, pp 3464–3470. [PubMed: 15875883]
35. Nandiyanto ABD; Suhendi A; Ogi T; Iwaki T; Okuyama K, Synthesis of additive-free cationic polystyrene particles with controllable size for hollow template applications. *Colloid Surf. Part A: Physicochem. Eng. Asp.* 2012, 396, pp 96–105.
36. Hench LL; West JK, The Sol-Gel Process. *Chem. Rev.* 1990, 90 (1), pp 33–72.
37. Shi Y; Takai C; Fuji M, Facile synthesis of hollow silica nanospheres employing anionic PMNAA templates. *J. Nanoparticle Res.* 2015, 17 (204), pp 1–10.

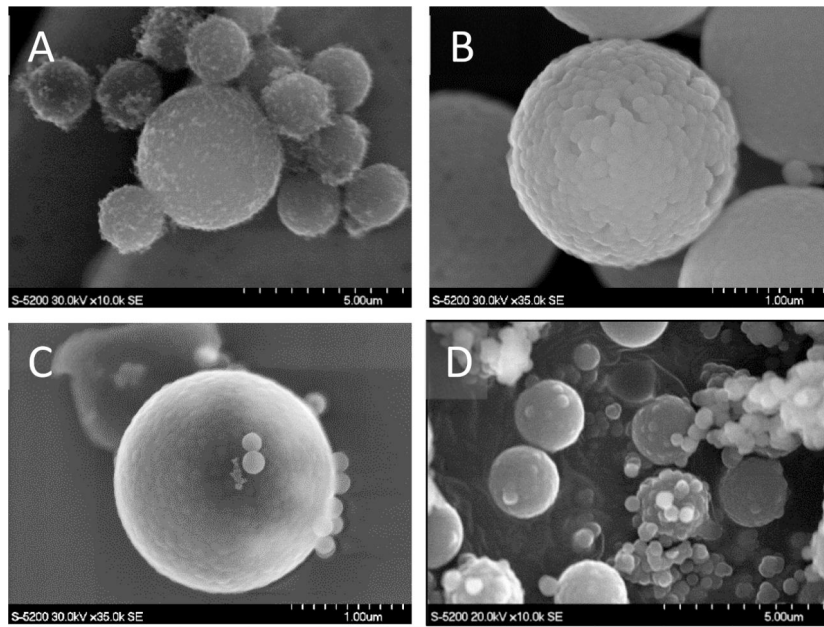


Figure 1. SEM images of increasing TEOS concentration. 3 mL (1.a), 6 mL (1.b), 7.5 mL (1.c), 15 mL (1.d) TEOS/g PSM. All samples prepared in one-pot synthesis at 1 mL NH_4OH /1 mL TEOS.

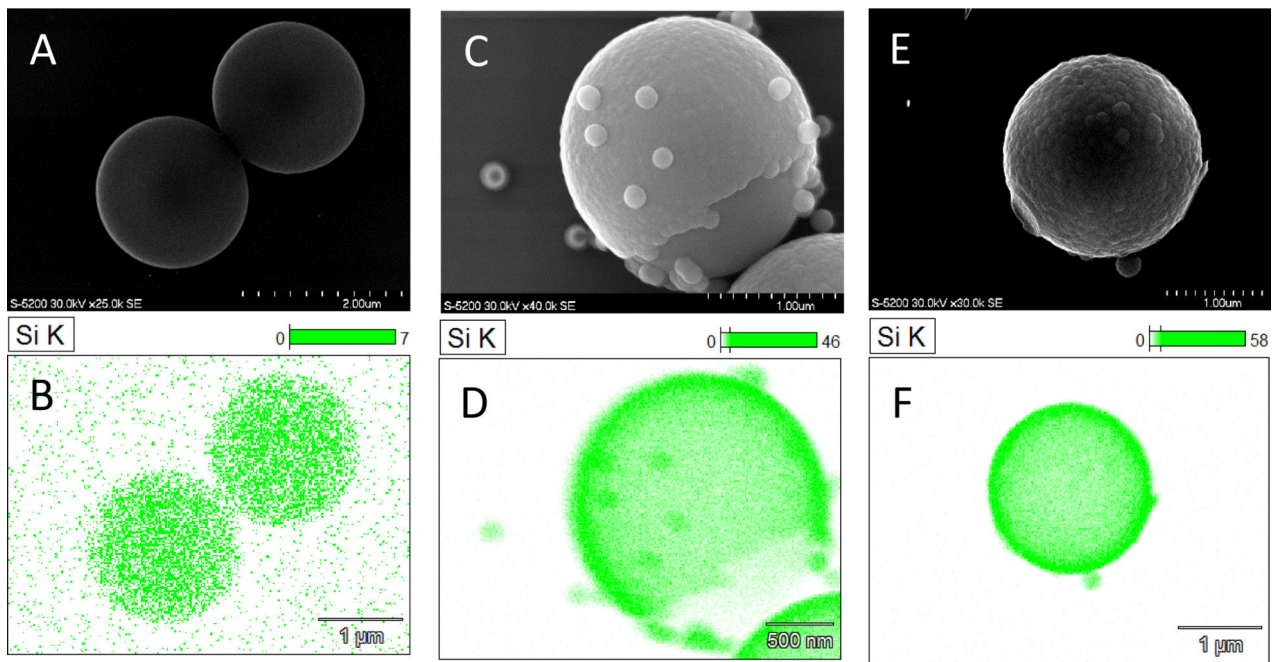


Figure 2. SEM images of silica shells formed under increasing concentrations of ammonium hydroxide. Concentrations varied from 0.5 mL (A-B), 1 mL (C-D), and 2 mL (E-F) NH_4OH /1 mL TEOS. All samples were prepared with 6mL TEOS/g PSM in a one-step synthesis on anionic PSM's.

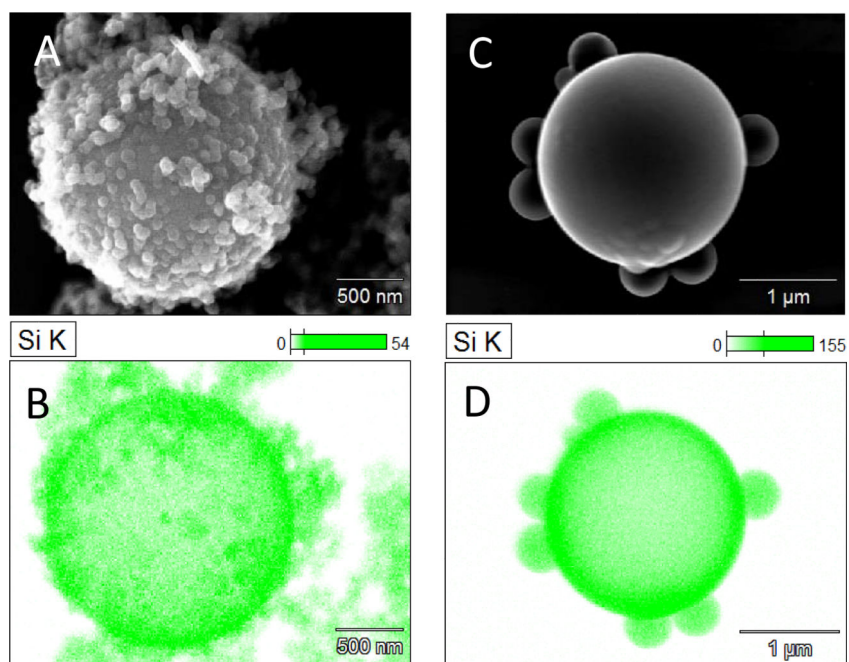


Figure 3. SEM images of silica shells formed on cationic PSM's. PS was functionalized with PDADMAC concurrently (A-B) or prior (C-D) to silica shell coating process. TEOS concentrations varied from 6 mL (A/B) to 7.5 mL (C/D) per 1 g PSM. NH_4OH was varied from 1mL (A/B) to 1.5mL (C/D) per 1 mL TEOS. Samples (3.A-D) were prepared in one-increment reactant introduction.

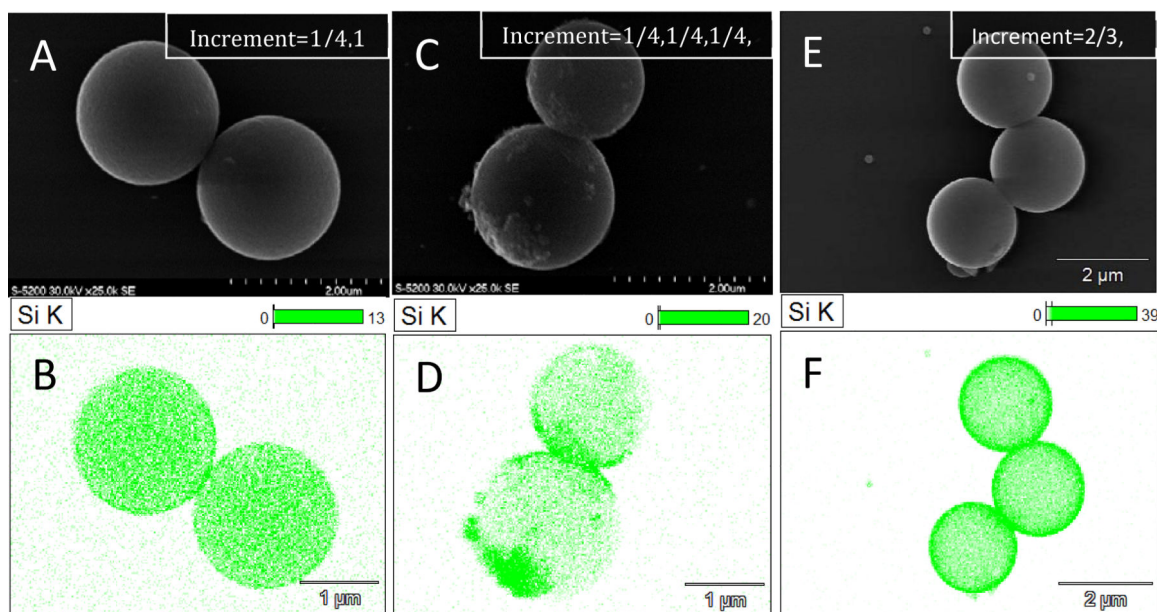


Figure 4.

A,B: Thin, smooth silica shell resulting from two additions of $\frac{1}{4}$ reactant addition. C,D: Asymmetric, partially smooth silica shells resulting from full $\frac{1}{4}$ reactant addition. E,F: Thick smooth silica shells formed from two additions ($\frac{2}{3}$ followed by $\frac{1}{3}$). All particles were coated in PDADMAC and used baseline TEOS/ NH_4OH bulk reactant ratios (6 mL TEOS: 1 g PSM and 1.5 mL NH_4OH : 1 mL TEOS).

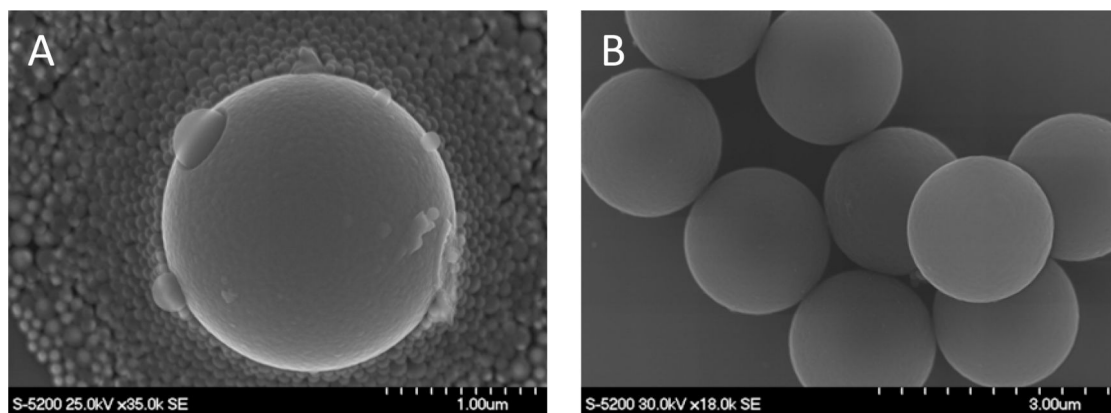


Figure 6.

A: PDADMAC-coated PS particle after two increments of $\frac{1}{2}V_{\text{total}}$ with many colloids in solution and in contact with the particle. Sample was removed from solution, frozen, and immediately imaged. B: After the particles from (A) have been fully reacted and processed via centrifugation. The silica colloids from (A) are no longer present.

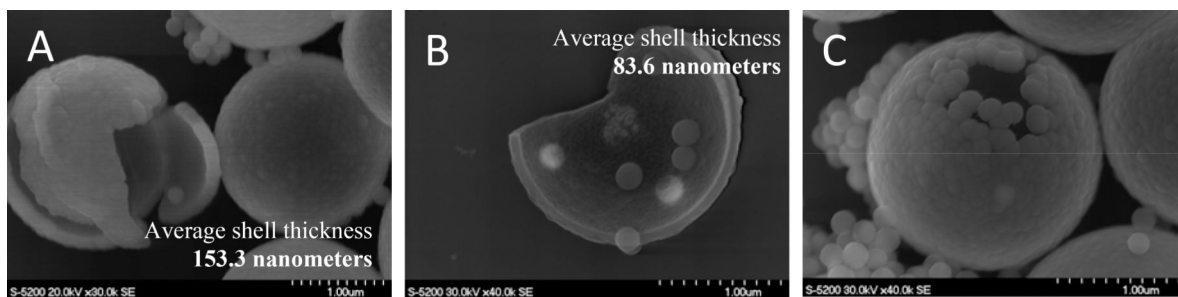
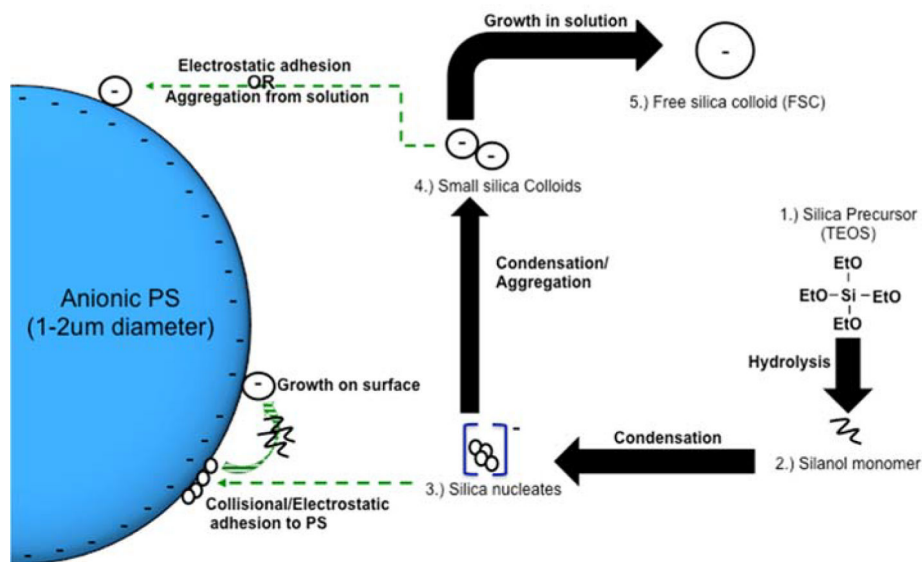


Figure 7.

A-C: RL shells formed from conditions identical to those utilized to generate the particles in Figure 1B, which were subsequently calcined via a 10°C/min ramp speed, isothermally held at 450°C for 2 hours, and a ramp down to room temperature via ambient cooling.

**Scheme 1.**

Graphical representation of silica shell formation on an anionic polystyrene core via the sol-gel process

Table 1.

Summary of synthetic sol-gel reaction parameter optimization trials.

	mL TEOS/g PSM	mL NH ₄ OH/mL TEOS	Shell Character	Image (Figure.Subfigure)
Trial 1	3	1	Incomplete/fuzzy	1.A
Trial 2	6	1	RL	1.B
Trial 3	7.5	1	RL [*] w/ colloids	1.C
Trial 4	15	1	RL [*] w/ colloids	1.D
Trial 5	6	0.5	No shell	2.A–B
Trial 6	6	1	RL [*]	2.C–D
Trial 7	6	2	RL [*] w/ colloids	2.E–F

*Raspberry-like (RL)